LAWRENCE
LIVERMORE
NATIONAL
LABORATORY

LLNL-TR-649567

Rapid Debris Analysis Project Task 3 Final Report - Sensitivity of Fallout to Source Parameters, Near-Detonation Environment Material Properties, Topography, and Meteorology

P. Goldstein

February 11, 2014

Disclaimer

This work performed under the auspices of the U.S. Department of Energy by Lawrence Livermore National Laboratory under Contract DE-AC52-07NA27344.

Defense Threat Reduction Agency
8725 John J. Kingman Road, MS 6201
Fort Belvoir, VA 22060-6201

DTRA-TR-XX-XX

(For J9-NTF: Technical Report # assigned by J9-NTF during review process)

TECHNICAL REPORT

Rapid Debris Analysis Project

Task 3 Final Report –

Sensitivity of Fallout

to Source Parameters, Near-Detonation

Environment Material Properties,

Topography, and Meteorology

Approved for public release; distribution is unlimited.

February 2014

DTRA01-XX-X-XXXX (See contract documents)

Authored by:

Peter Goldstein, Ph.D.

Prepared by:

Lawrence Livermore National Laboratory
PO Box 808
Livermore, CA 94551

DESTRUCTION NOTICE

Destroy this report when it is no longer needed. Do not return to sender.

PLEASE NOTIFY THE DEFENSE THREAT REDUCTION AGENCY, ATTN: OP-ONIUI, 8725 JOHN J. KINGMAN ROAD, MS-6201, FT BELVOIR, VA 22060-6201, IF YOUR ADDRESS IS INCORRECT, IF YOU WISH IT DELETED FROM THE DISTRIBUTION LIST, OR IF THE ADDRESSEE IS NO LONGER EMPLOYED BY YOUR ORGANIZATION.

REPORT DOCUMENTATION PAGE

Form Approved
OMB No. 0704-0188

1. REPORT DATE *(DD-MM-YYYY)*	2. REPORT TYPE	3. DATES COVERED *(From – To)*
06-02-2014	Technical	–

4. TITLE AND SUBTITLE
Rapid Debris Analysis Project Task 3 Final Report: Sensitivity of Fallout to Source Parameters, Near-Detonation Environment Material Properties, Topography, and Meteorology

5a. CONTRACT NUMBER
Example: F33615-86-C-5169

5b. GRANT NUMBER
Example: AFOSR-82-1234

5c. PROGRAM ELEMENT NUMBER
Example: 61101A

6. AUTHOR(S)
Peter Goldstein, Ph.D.

5d. PROJECT NUMBER
Example: 1F665702D1257; ILIR

5e. TASK NUMBER
Example: 05, RF0330201; T4112

5f. WORK UNIT NUMBER
Example: 001, AFAPL30480105

7. PERFORMING ORGANIZATION NAME(S) AND ADDRESS(ES) AND ADDRESS(ES)
Ex: DTRA, OP-ONIU

8. PERFORMING ORGANIZATION REPORT NUMBER
LLNL-TR-XXXXXX

9. SPONSORING / MONITORING AGENCY NAME(S) AND ADDRESS(ES)
Ex: DTRA

10. SPONSOR/MONITOR'S ACRONYM(S)
Ex: DTRA

11. SPONSOR/MONITOR'S REPORT NUMBER(S)

12. DISTRIBUTION / AVAILABILITY STATEMENT

This work performed under the auspices of the U.S. Department of Energy by Lawrence Livermore National Laboratory under Contract DE-AC52-07NA27344.

13. SUPPLEMENTARY NOTES

Ex: This work was sponsored by the Defense Threat Reduction Agency under RDT&E RMC.

14. ABSTRACT

This report describes the sensitivity of predicted nuclear fallout to a variety of model input parameters, including yield, height of burst, particle and activity size distribution parameters, wind speed, wind direction, topography, and precipitation. We investigate sensitivity over a wide but plausible range of model input parameters. In addition, we investigate a specific example with a relatively narrow range to illustrate the potential for evaluating uncertainties in predictions when there are more precise constraints on model parameters.

15. SUBJECT TERMS

Term Term Term Term Term

16. SECURITY CLASSIFICATION OF:			17. LIMITATION OF ABSTRACT	18. NUMBER (of pages)	19a. NAME OF RESPONSIBLE PERSON
a. REPORT	b. ABSTRACT	a. THIS PAGE	Ex: SAR	31	Ex: J. Rowell
UNCLASS	UNCLASS	UNCLASS			19b. TELEPHONE NUMBER (include area code) Ex: 202-555-5555

Standard Form 298 (Rev. 8-98)
Prescribed by ANSI Std. Z39.18

CONVERSION TABLE

International System of Units of Measurement

MULTIPLY TO GET	BY BY	TO GET DIVIDE
Angstrom	1.000 000 x E-10	meters (m)
Atmosphere	1.012 25 x E +2	kilo pascal (kPa)
Bar	1.000 000 x E + 2	kilo pascal (kPa)
Barn	1.000 x E – 28	meter^2 (m^2)
British thermal unit (thermochemical)	1.054 350 x E + 3	joule (J)
calorie (thermochemical)	4.184 000	joule (J)
cal (thermochemical)/cm^2	4.184 000 x E-2	mega joule/m^2 (MJ/m^2)
Curie	3.7000 000 x E + 1	giga becquerel (GBq)*
degree (angle)	1.745 329 x E – 2	radian (rad)
degree (Fahrenheit)	Tk = (t +459.69)/1.8	degree kelvin (K)
electron volt	1.602 19 x E – 19	joule (J)
Erg	1.000 000 x E – 7	joule (J)
erg/sec	1.000 000 x E – 7	watt (W)
Foot	3.048 000 x X-1	meter (m)
foot-pound-force	1.355 818	joule (J)
gallon (U.S. liquid)	3.785 412 x E – 3	meter^3 (m^3)
Inch	2.540 000 x E -2	meter (m)
Jerk	1.000 000 x E + 9	joule (J)
joule/kilogram (J/kg) (absorbed dose)	1.000 000	Gray (Gy)**
Kilotons	4.183	Terajoules
kip (1000 lbf)	4.448 222 x E + 3	newton (N)
kip/inch^2 (ksi)	6.894 757 x E +3	kilo pascal (kPa)
Ktap	1.000 000 x E +2	newton-second/m^2 (N-s/m^2)
Micron	1.000 000 x E – 6	meter (m)
Mil	2.540 000 x E – 5	meter (m)
mile (international)	1.609 344 x E + 3	meter (m)
Ounce	2.834 952 x E – 2	kilogram (kg)
pound-force (lbf avoirdupois)	4.448 222	newton (N)
pound-force inch	1.129 848 x E – 1	newton-meter (N*m)
pound-force/inch	1.751 268 x E + 2	newton-meter (N/m)
pound-force/foot^2	4.788 026 x E – 2	kilo pascal (kPa)
pound-force/inch^2 (psi)	6.894 757	kilo pascal (kPa)
pound-mass-foot^2 (moment of inertia)	4.214 011 x E – 2	kilogram-meter^2 (kg*m^2)
pound-mass/foot^3	1.601 846 x E + 1	kilogram/m^3 (kg/m^3)
rad (radiation absorbed dose)	1.000 000 x E – 2	Gray (Gy) **
rem (roentgen equivalent man)		Sievert (Sv) ***
Roentgen	2.579 760 x E – 4	coulomb/kilogram (C/kg)
Shake	1.000 000 x E – 8	second (s)
Slug	1.459 390 x E + 1	kilogram (kg)
Torr (mm Hg, 0 degrees C)	1 333 22 x E – 1	kilo pascal (kPa)

* *The Becquerel (Bq) is the SI unit of radioactivity: 1 Bq = 1 event/s.*
** *The Gray (Gy) is the SI unit of absorbed radiation.*
*** *The Sievert (SV) is the SI unit of dose equivalent.*

TABLE OF CONTENTS

LIST OF FIGURES

LIST OF TABLES

SUMMARY

This report describes the sensitivity of predicted nuclear fallout to a variety of model input parameters, including yield, height of burst, particle and activity size distribution parameters, wind speed, wind direction, topography, and precipitation. We investigate sensitivity over a wide but plausible range of model input parameters. In addition, we investigate a specific example with a relatively narrow range to illustrate the potential for evaluating uncertainties in predictions when there are more precise constraints on model parameters.

The objective of this work is to provide information on the range of model generated nuclear fallout patterns that can be expected for a plausible range of input parameters so that we can develop a better understanding of how uncertainties in specific scenario model parameters translate into uncertainties in that scenarios predicted fallout.

In this project, we have divided our analysis into three parts, in the first we focused on sensitivity to the yield and height of burst of an event. Next we evaluated the sensitivity to the models description of the near source environment. We varied the particle activity-size distribution to model variations in the soil environment near the detonation, because the soil particle size distributions determine the activity-size distributions, which, in turn, determines how activity is distributed spatially in the stabilized fallout cloud and how quickly that activity will fallout as it is transported and diffused downwind.

In the final phase of this work, we investigated the sensitivity of fallout to meteorological parameters including wind speed and direction, topography, and precipitation. Our analysis began with a baseline simulation for an actual event, the Nevada Test Site explosion Johnnie Boy that had a yield of one-half a kiloton and a depth of burst of approximately one-half meter. The initial meteorological conditions were based on observations reported in Hawthorne (1979) near ground zero. Local topography was based on GTOPO30 digital elevation data from the US Geological Survey.[1]

Model parameters were allowed to vary over a relatively large but plausible range of values and a specific example with relatively narrow range of model parameters was considered to illustrate how uncertainties in model predictions might be evaluated when there are better constraints on model parameters. We did not attempt an extensive investigation into trade-offs due to simultaneous variations in multiple model parameters because of the large number of simulations that would have been required and the potential complexity involved in interpreting such data. However, we did observe some clear indications that there were significant trade-offs between parameters like yield and height-of-burst and median particle-size and the geometric standard deviation of the particle-size distribution. We also observed that the sensitivity to topography was a function of yield and meteorological conditions.

1. http://eros.usgs.gov/#/Find_Data/Products_and_Data_Available/gtopo30_info

In the course of this work, we have also developed tools that would allow us to rapidly produce more specific results given a specific detonation scenario and better constrained ranges for the model input parameters.

The primary results from this study are as follows:

1. Fallout levels are non-linear functions of yield and height of burst with greater variation in levels at lower yields and smaller heights of burst.
2. Potential variations in fallout associated with the uncertainties in the in-situ environmental material properties, i.e., the size of soil particles that carry radioactivity, and the particle activity-size distribution model are potentially quite large. Our simulations with plausible but poorly constrained distributions produced cases ranging from the majority of fallout being deposited near ground-zero to those where the majority of material was transported to relatively large distances downwind.
3. Better constraints on the in-situ particle size distribution model parameters, particularly at low yields and heights of burst, are critical for producing reliable estimates of nuclear detonation fallout.
4. Uncertainties in meteorology are another potentially significant source of uncertainty in predicted fallout. For example, variation in wind direction as a function of height can lead to complicated, potentially multi-lobed, fallout footprints. Such footprints are consistent with observations of fallout at the Nevada Test Site.
5. Variations in wind speed as a function of height can have a significant effect on the relative amount of material that is deposited in the near source and downwind regions.
6. Precipitation scavenging can significantly increase ground deposition in areas of precipitation, and, then, reduce deposition downwind of the precipitation areas.
7. Topography can cause additional complexity in the fallout plumes, changing the direction of the plume, causing enhanced deposition on elevated terrain, and changing the distances at which significant fallout occurs.
8. Fallout sensitivity to topography depends on yield as well as local meteorology.

PREFACE

The objective of this work is to utilize LLNL's National Atmospheric Release Advisory Center (NARAC)[2] fallout modeling capabilities to improve our understanding of the sensitivity of fallout patterns to detonation parameters, environmental material, and meteorology so that the uncertainty of results from models can be estimated when used in exercises or real events. As we gain confidence in our estimates of input model parameters, results may become useful for developing reliable, cost-effective detection networks and sampling/collection strategies.

2. The NARAC capabilities are the primary federal radiological/nuclear plume modeling capabilities utilized by the Interagency Modeling and Atmospheric Assessment Center (IMAAC). NARAC supplies these predictions to the Department of Energy (DOE) and the Department of Homeland Security (DHS) IMAAC Operations hub at DTRA.

THIS PAGE IS INTENTIONALLY LEFT BLANK.

1.0 INTRODUCTION

In this project, we used the NTS explosion Johnnie Boy as our baseline simulation because it has relatively well established and openly available detonation parameters and meteorology (DOE NV-209, 1997; Hawthorne, 1979). This event is also of particular interest because it is a low-yield, near-surface event which is consistent with plausible nuclear terrorism scenarios (e.g., May et al, 2008). The near source materials parameterization and topography of the Nevada Test Site are also reasonably well known (e.g., Tompkins, 1968, Heft, 1970, Spriggs, 2012). A number of authors have also used this event when evaluating fallout models (e.g., Norment, 1979, Martin, 1983, McGahan, 2001, Morris, 2004).

Extensive work has been done to develop, verify, validate, and compare fallout models and their components (e.g., Huebsch, 1966, Norment, 1979, Bridgeman, 1982, Harvey et al, 1992, McGahan, 2001). However, relatively little has work has been done to evaluate the sensitivity of such models. Relevant sensitivity studies include Tompkins (1971) and McGahan (1974).

The work by McGahan (1974) is particularly relevant because he looked at the sensitivity of fallout to some of the same parameters examined here. Key differences are the range of yields examined, which are relatively low in this study, ranging from sub-kiloton to tens of kilotons and were relatively high in McGahan's study (30kt to 10 Mt). McGahan also investigated sensitivity to particle activity-size distribution but only considered the effect of utilizing different size-distribution models (e.g., Freiling, 1961, Tompkins, 1968) without varying the carrier material (e.g., soil particles) parameters. McGahan's work also used constant meteorology and did not allow for variations in terrain elevation. Despite these differences and the use of older technology, McGahan's study is a useful resource for evaluating some of the potential sources of uncertainty in model output, particularly at higher yield.

For example, McGahan found that the sensitivity of fallout to yield was quite linear with peak amplitudes of groundshine dose and dose rates varying in proportion to yield. In contrast, we have found variations in amplitude as well as plume size and shape that could not be predicted as a simple linear function of yield, especially at low yields. McGahan also found significant sensitivity to the analytic form used to describe the particle activity-size-distribution, as well as the choice of a refractory vs volatile size-distribution. This is consistent with our modeling where we also consider refractory and volatile distributions and different model parameterizations. In addition to these model sensitivities, we show that there is great deal more uncertainty when potential variations in the size-distribution parameters are taken into account.

In our analysis of sensitivity to yield and height of burst (Goldstein, 2013a) we found significantly higher sensitivity of fallout to variations in yield and height of burst for lower yields and heights-of-burst, as well as a yield-dependent sensitivity to local topography. In our analysis of the sensitivity of fallout to the near-detonation environment—as represented by the in-situ carrier material (e.g., soil) particle size distribution and fallout debris activity-size distribution—as median particle size is increased from one test case to the next, the particle settling velocities increase accordingly, resulting in more rapid fallout. Therefore, the fallout ground concentration closer to the detonation location will tend to increase with increasing median particle size.

However, the downwind distances at which this increased ground concentration occurs varies, since it is a function of the wind speed, the particle-size-dependent settling velocities, and the activity-height distribution (which is a function of yield and height of burst).

In this report, we describe results from our analysis of the sensitivity of fallout to meteorology. We focus on the sensitivity to changes in wind direction as a function of height, and also investigate sensitivity to changes in wind speed as a function of height. We show that changes in wind direction with height of 30 degrees or more can cause significant changes in fallout and that these changes can be exacerbated by variations in the local topography. We note that such variations in meteorology are fairly common and suggest that they will need to be accounted for in order to make reliable predictions of fallout.

2.0 METHODS, ASSUMPTIONS, AND PROCEDURES

In this work we utilized LLNL's National Atmospheric Release Advisory Center (NARAC) fallout modeling capabilities to simulate fallout. The models we use include GRIDGEN (Walker, 2006), which is a tool for generating the horizontal/vertical grid mesh and terrain elevations needed by NARAC's meteorological data assimilation tool, ADAPT (Sugiyama et al., 2006), which in turn is used to build gridded descriptions of the mean wind fields and turbulence fields for NARAC's LODI (Nasstrom et al., 2007) Lagrangian particle simulation code that is used to transport, diffuse and deposit the fallout debris.

The nuclear detonation initial fallout debris source description in LODI that was used in this study is based on the source developed for the KDFOC fallout model (Harvey et al., 1992). This source description provides the initial particle activity-size distribution and the spatial distribution of activity that is used to define the initial activity and height distribution of the LODI marker particles. The KDFOC model is based on empirical observations of fallout from nuclear explosions at the Nevada Test Site (NTS).

Post-processing of the transported and deposited material is performed by NARAC's BIN software which allows a variety of mathematical procedures to be applied to the LODI (Nasstrom et al., 2007) output including mathematical operations such as addition, subtraction, multiplication and division as well as scaling and time-integration.

In this work, we focused on sensitivity analysis for relatively low yields ($y<10$ kt) and heights of burst ($hob<100$ m) because they are of particular concern for scenarios involving nuclear terrorism (e.g., May et al., 2008). The range of parameters for the in-situ environmental material properties (particle-size distributions of carrier material such as soil) were chosen so that they encompassed possible near-detonation environmental materials with relatively small median diameters and geometric standard deviations (such as in an air-burst or finer soil particle) and materials with relatively large median diameter and geometric standard deviation in the particle size distribution (such as in coarser soil). A detailed description of the methods for computing the particle activity-size distributions is provided in Goldstein (2013b). Meteorological variations included changes in wind direction over a full 360 degrees and changes in wind speed by a factor of two above and below the baseline wind profile. Sensitivity to topography became apparent when we varied the wind direction because the topography varied as a function of the azimuth angle of transport from ground zero.

3.0 RESULTS AND DISCUSSION

In this section, we summarize results from our previous reports, show new results from our constrained yield and height-of-burst simulation, and describe new results on the sensitivity of nuclear detonation fallout to meteorology and topography.

Figure 3-1 illustrates the potential sensitivity of fallout to yield and height-of-burst over the relatively broad yield range of 0.1 to 10 kt and 0 to 100 m height of burst. As noted previously there are large variations in the predicted fallout over this range and the variations are more rapid at lower yields and heights of burst. It is also clear that the fallout plume is bifurcating at larger yields and we note that this can be explained in terms of the greater height of the initial fallout cloud, the rotation of the wind direction towards the northeast at increasing heights, and the inability of the lower yield plumes to rise above the local topography towards the northeast of the detonation point.

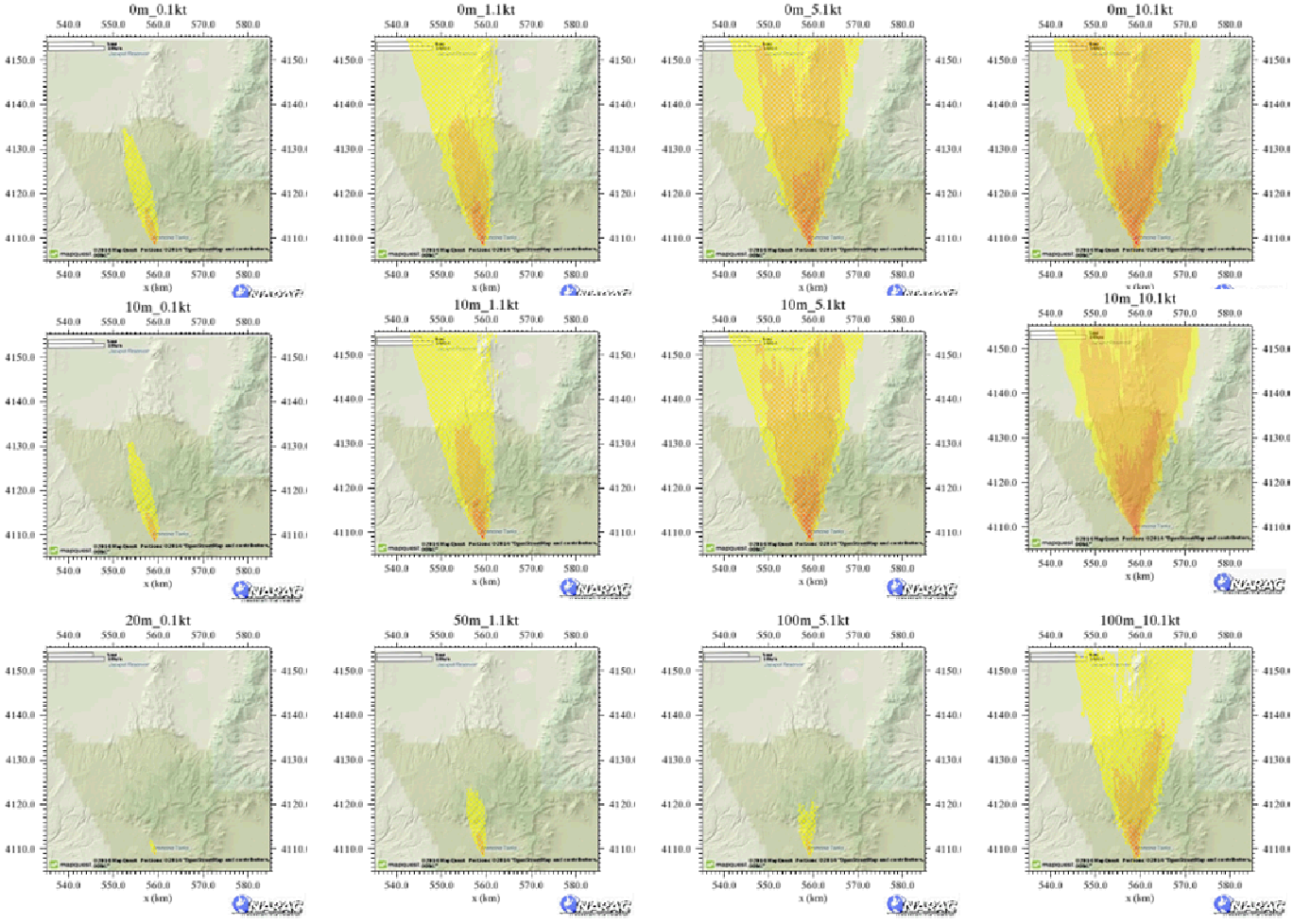

Figure 3-1: Ground-shine dose as a function of yield and height of burst. Height of burst and yield are indicated at the top of each subplot (e.g., "0m_0.1kt"); yield increases from left to right, and height of burst increases from top to bottom. Each subplot shows

accumulated groundshine dose contours after 96 hrs. The outermost contour (outer edge of yellow region) corresponds to 1 R. Adjacent contours differ by a factor of 10 and increase toward the vicinity of the detonation point indicated by the innermost contour. The contours overlay the NTS topography in the vicinity of the Johnnie Boy test. Each plot is approximately 50 km on a side. The assumed detonation location is in the center and south end of the mapped area.

Table 3.1 and Figure 3.2 show results for a narrower range of yield (0.2 to 1.6 kt) and height-of-burst (0 to 20 m) parameters to illustrate the potential uncertainty in predicted fallout of a better constrained scenario. As expected for this smaller range of yields and heights-of-burst, the range of variation is much smaller. However, there are still noteworthy variations from simple linear trends. For example, there is a rapid drop off in peak fallout groundshine dose with height-of-burst, between 10 and 20 m, as we move to lower yields. This can be seen in the last column in Table 3.1 which contains the ratio of the peak dose for that yield and height-of-burst divided by the peak dose of the y=0.2, hob=20 simulation. Note how the ratio decreases rapidly above 10 m for the low yield (0.2 and 0.4 kt) cases. This is consistent with the decreasing size of the fallout footprints, with increasing height-of-burst in Figure 3.2. Another feature that is visible in Figure 3.2 is the effects of topography as we move to higher yields. At higher yields the initial fallout cloud will rise and stabilize at greater heights, allowing a greater proportion of material to be transported above and beyond the local topography and fallout further downwind. This may explain the broader footprint that appears as we increase the initial yield. Based on Figure 3.2, it appears that yields as low as 0.8 kt may be sufficient to increase the height of the stabilized cloud enough that significant material can be transported over the local topography.

Table 3-1. Peak dose and the ratio of the peak dose to the peak dose of the y=0.2, hob=20 simulation.

Name	Yield, y (kt)	Height of Burst, hob (m)	Max. Dose	Dose Ratio to y=0.2, hob=20 dose
y0.2hob0	0.2	0	8,038	5.03
y0.2hob10	0.2	10	6,213	3.89
y0.2hob20	0.2	20	1,597	1
y0.4hob0	0.4	0	16,408	10.28
y0.4hob10	0.4	10	11,234	7.03
y0.4hob20	0.4	20	4,549	2.85
y0.8hob0	0.8	0	25,441	15.93
y0.8hob10	0.8	10	18,134	11.36
y0.8hob20	0.8	20	11,917	7.46
y1.6hob0	1.6	0	49,953	31.28
y1.6hob10	1.6	10	34,995	21.91
y1.6hob20	1.6	20	18,428	11.54

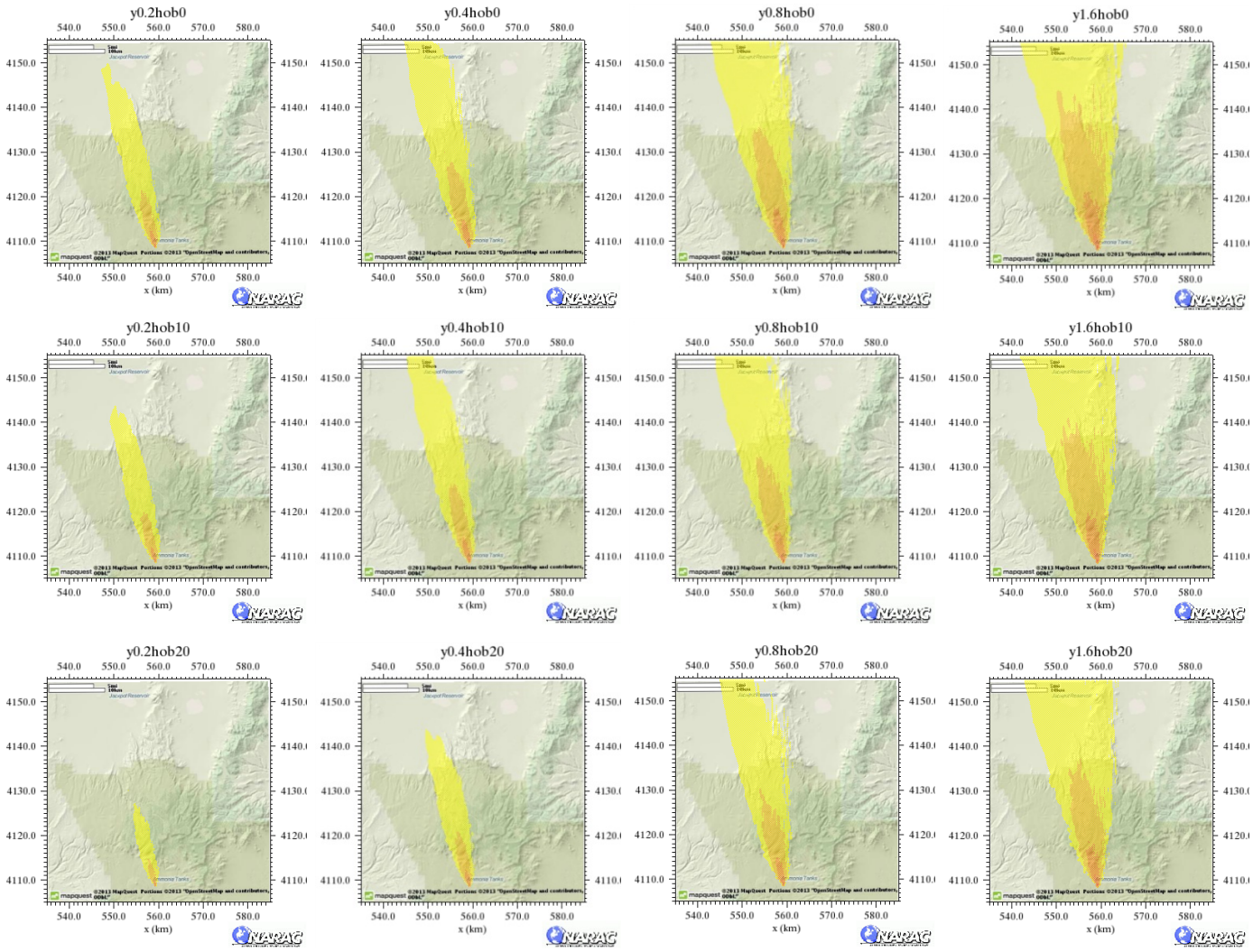

Figure 3-2. Ground-shine dose for a narrower range of yield and height of burst than that shown in Figure 3-1. Yield and height of burst are indicated at the top of each subplot; yield increases from left to right, and height of burst increases from top to bottom.

Figures 3-3, 3-4, and 3-5 are repeated here from our previous report (Goldstein, 2013b) on the sensitivity to in-situ environmental (e.g., soil) material properties. Figures 3-3 and 3-4 depict the range of activity size distributions used in our simulations and Figure 3-5 shows the corresponding plumes for these simulations. The ranges for the activity-size-distributions are quite large but seem plausible given the relatively small range of median diameters and geometric standard deviations they are based on. The chosen ranges are also useful because they produce a wide range of fallout plumes including ones that deposit almost all the fallout material near ground zero, and others where the majority of material is transported to large downwind distances. The range of particle size distributions accounts for potential differences between volatile and refractory material and considers differences in the particle activity-size distribution between Freiling's original radial power law (1961) and the modified radial power law developed by Tompkins (1968).

Considering the wide range of fallout in Figure 3-5, we suggest that uncertainties in predicted nuclear-detonation fallout will be quite large in regions where we have limited knowledge of the in-situ environmental material properties, and/or in cases in which there is uncertainty in the methods of estimating the fallout debris particle activity-size distribution.

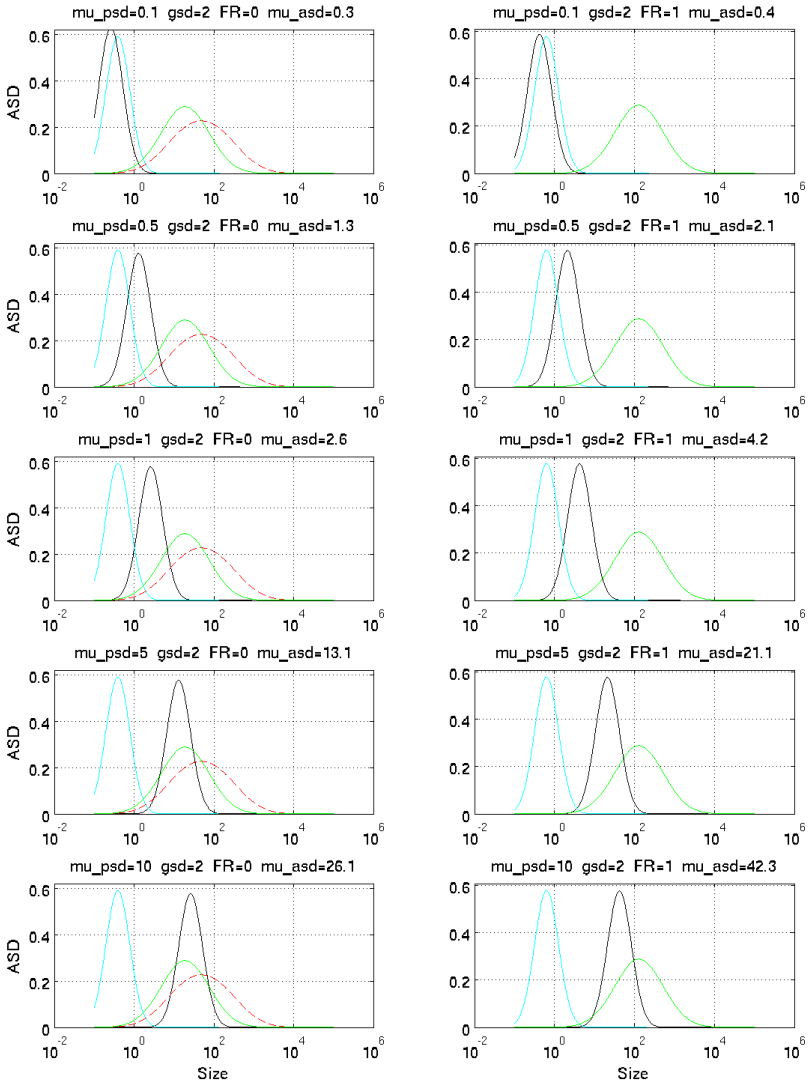

Figure 3-3. Activity-size distributions (ASD) (solid-black curves) as a function of particle size (radius in μm) corresponding to particle number-size distributions with median radii ranging from 0.1 to 10 microns. The median of the number-particle distribution and of the activity-size distribution are indicated at the upper left and right of each plot, respectively. The geometric standard deviation (GSD) is two. Distributions corresponding to surface distributed activity (FR=0) and volume distributed activity (FR=1) are plotted in the left- and right-hand columns, respectively. Plots of the default ASD used by DELFIC for an air-burst (cyan curve) and two DELFIC options for near-surface burst at NTS (green and red curves) are shown for reference.

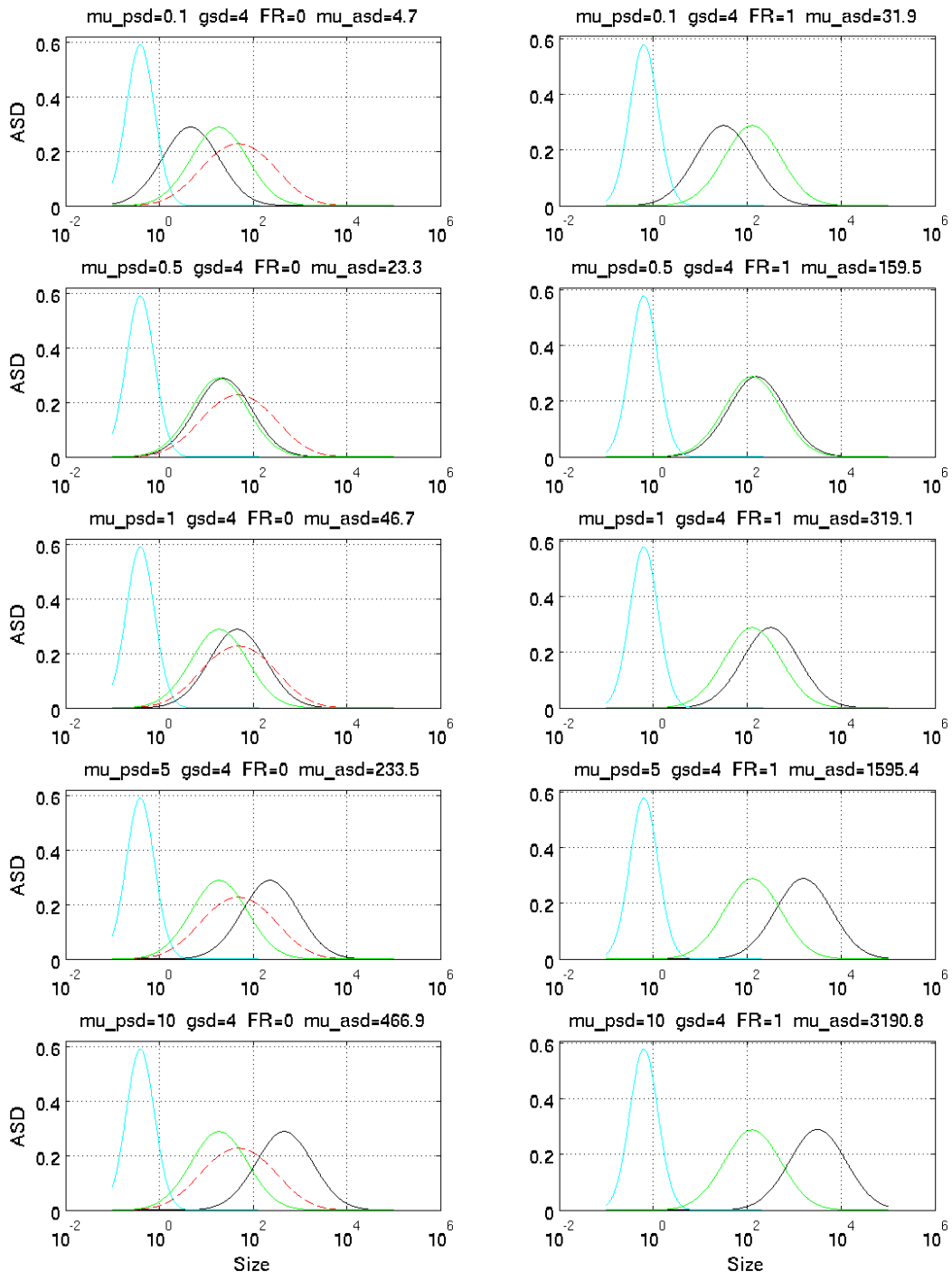

Figure 3-4. Same as Figure 3-3, except geometric standard deviation (GSD) is four.

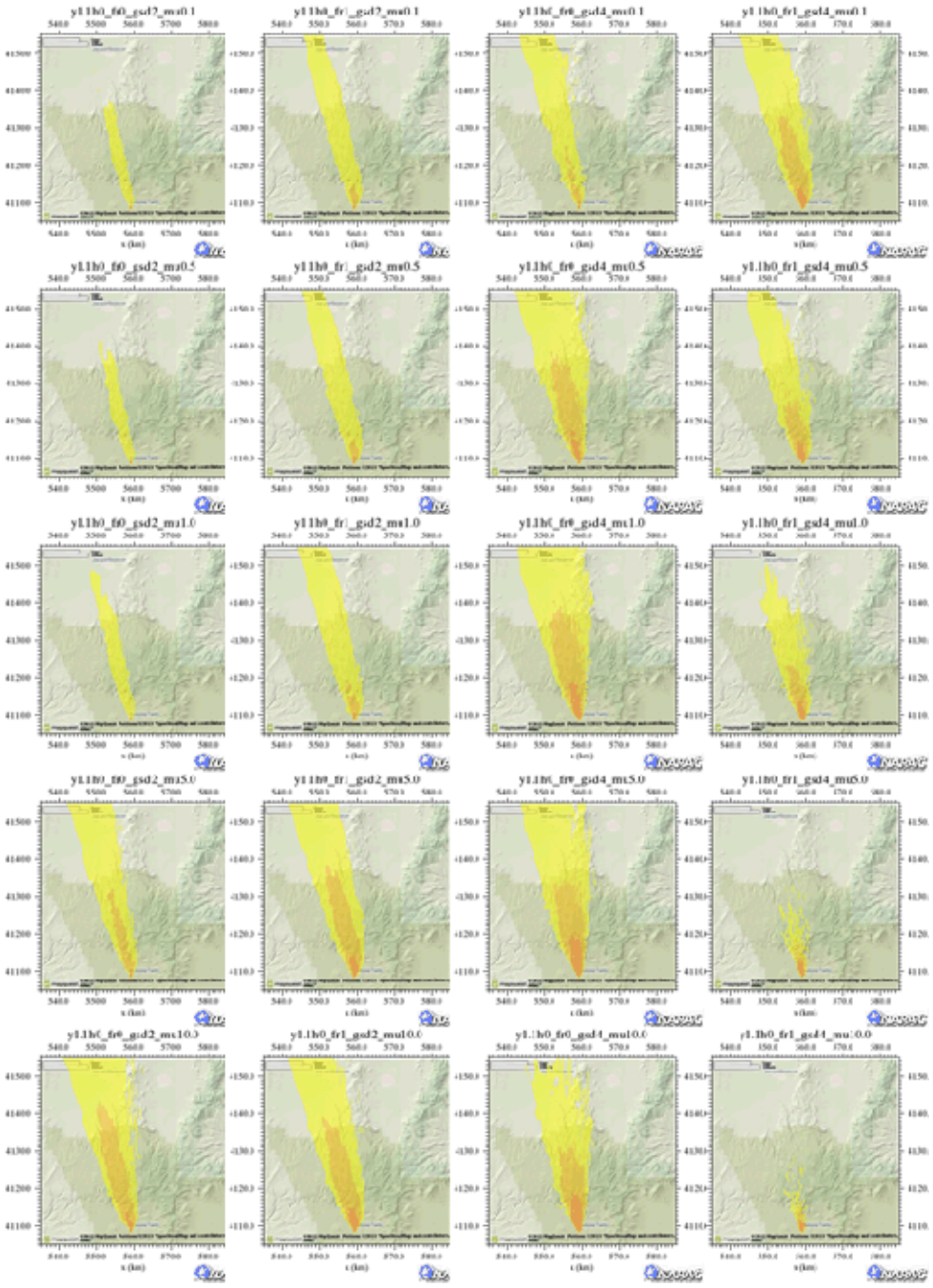

Figure 3-5. **Ground-shine dose contours corresponding to the activity-size distributions shown in Figure 3-1 (left two columns) and 3-2 (right two columns). Each subplot shows accumulated ground-shine dose contours after 96 h. The outermost contour (outer edge of yellow region) corresponds to 1 R. Adjacent contours differ by a factor of 10 and increase toward the vicinity of the detonation point indicated by the innermost red contour. Plots corresponding to large median activity-size distribution radii have significantly higher dose levels, not shown by the contours, at ground zero. The contours overlay the NTS topography in the vicinity of the Johnnie Boy test. Each plot is 50 km on a side. The assumed detonation location is in the center and south end of the mapped area.**

To investigate sensitivity to changes in the horizontal wind direction with height (directional wind shear) we compared fallout from a model with a constant northward wind (our baseline profile) to a suite of models where the wind direction was rotated by a fixed angle above a fixed height. For any one wind profile, there were only two wind directions, with the transition between the two wind directions occurring at different heights. The amount of rotation was allowed to range from 30 to 330 degrees and the heights above which the rotation occurred ranged from roughly 300 to 2700 m above ground level in 300 m increments. The winds were also rotated at 3500 m above ground level. Table 3.2 lists an example wind profile. The example profile corresponds to a 60 degree rotation of the winds toward the northeast above the top height in the wind profile. The resulting fallout plume is shown in the upper left corner of Figure 3.6 and is titled ds_60_1. The fallout patterns for a wind profile with all the winds above the second highest level rotated toward the northeast is shown at the top center is and labeled ds_60_2. The remaining plots show fallout patterns for wind profiles where winds were rotated toward the northeast above successively lower levels.

Table 3.2: Example wind profile used to test the sensitivity to wind direction and speed. The wind profile listed corresponds to the plot in Figure 3.6 titled ds_60_1. In this example, winds above the top listed level was rotated 60 degrees toward the northeast. All the winds in the baseline profile were towards the north. We ran simulations for all the winds rotated above each level and for rotations ranging from 30 degrees to 330 degrees in 30 degree increments. Sensitivity to wind speed was investigated by increasing and decreasing the baseline profiles wind speeds by up to a factor of two (see text).

Height above ground (m)	Wind Direction (degrees)	Wind Speed (m/s)
259.08	180	4.2
563.88	180	5.13
868.68	180	5.74
1173.48	180	6.35
1478.28	180	6.96
1783.08	180	7.57
2087.88	180	8.18
2392.68	180	8.79
2697.48	180	9.39
3500	240	11

The resulting fallout patterns, for the full range of heights and angles of rotation, ranged from relatively simpler, narrower footprints, when the winds were approximately uni-directional, to wider, more-complex, sometimes two-lobed patterns when the wind had as little as a 30 degree rotation. Figure 3.6 illustrates the type of patterns we found using a rotation towards the northeast of 60°. In this example, as more of the winds were rotated from due north toward the northeast, by lowering the transition height between the two wind directions to successively lower heights, the footprint gradually widened from its initial northward direction into a two-lobed north-northeast plume and then narrowed into a plume toward the northeast. It also appears that the two-lobed patterns are caused by increased deposition on elevated terrain features, and less on lower terrain.

We also investigated the sensitivity of fallout to variations in wind speed with height and to precipitation. We found variations in wind speed with height had their greatest influence on the amount of fallout as a function of distance from the source (not shown). Not surprisingly, as wind speed was increased an increasing amount of fallout was distributed further downwind, as the downwind transport distance is greater in the time it takes material to settle to the ground. Although no attempt was made to investigate the sensitivity to simultaneous variations in wind speed and wind direction, it seems likely that more complicated fallout patterns could occur when both of these phenomena are acting at the same time.

Precipitation scavenging can have a significant effect on deposition patterns (e.g., Sugiyama et al., 2012). We investigated the sensitivity to precipitation by assuming a constant rain rate over the whole deposition period and varying the hourly precipitation rate between simulations from 0 to 2 mm/h in 0.2 mm/h increments. Results of our simulations (not shown) are consistent with the observations of Sugiyama et al. (2012) and suggest that precipitation scavenging can rapidly remove material from the fallout plume increasing the near-field deposition and reducing the downwind fallout footprint.

Some of the fallout patterns we observed (e.g., Figure 3-6) are relatively complicated given the relatively simple variations in the wind. It is not hard to imaging much more complicated fallout patterns given more complex meteorology and topography or interactions with man-made structures. The ground-shine dose rate from the NTS explosion TURK, Figure 3-7, which appears to have had relatively complicated meteorology (Hawthorne, 1979), is an example of the potential complexity.

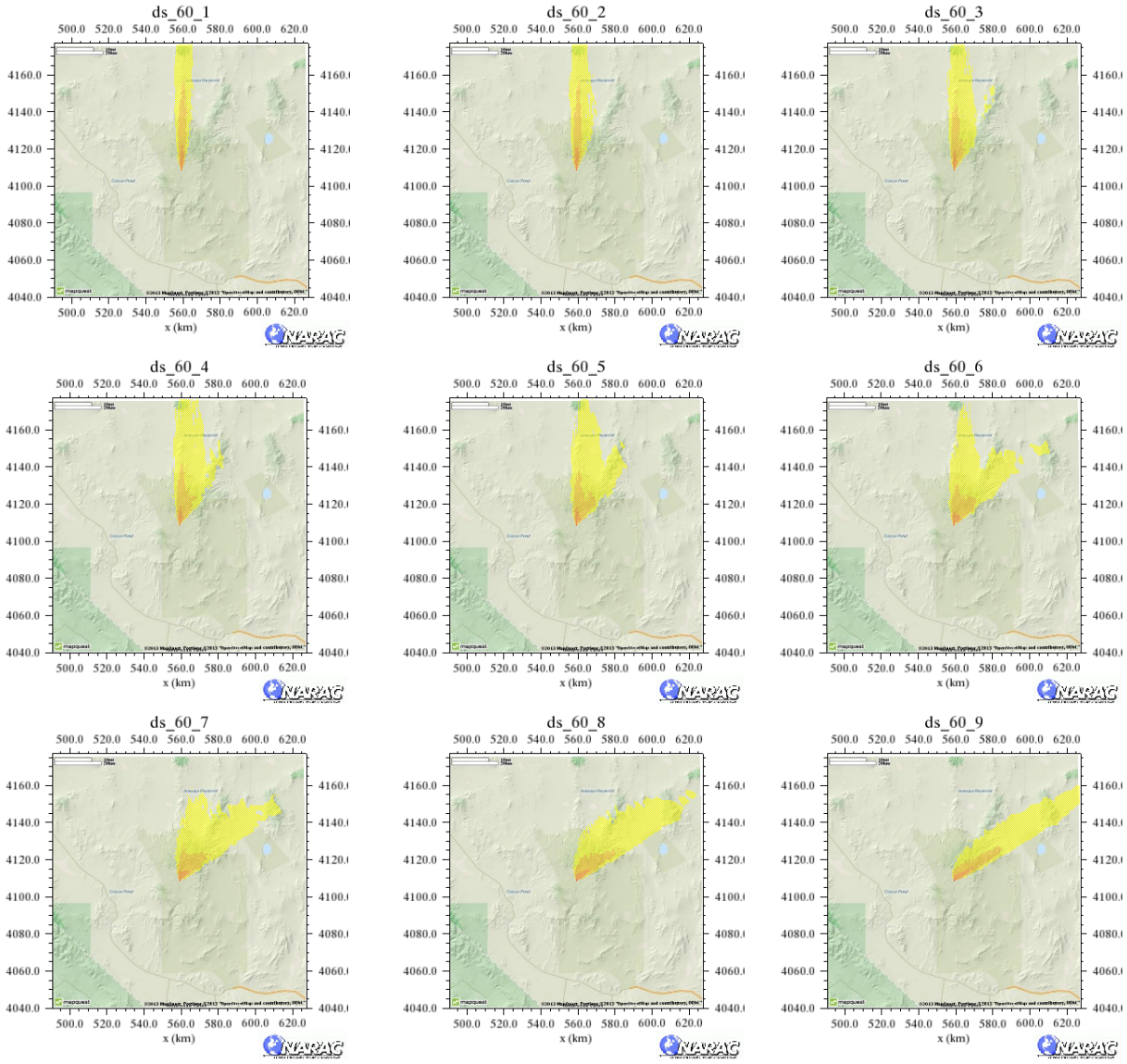

Figure 3-6. Ground-shine dose for 60° horizontal wind shear above successively lower elevations from ground level. The height of the wind shear decreases approximately 300 m from plot to plot with successive levels indicated by the integer at the end of the plot title. All the simulations used a yield of 1.1 kt and a surface (0 m) height-of-burst. Note the broadening and then narrowing of the plume as the majority of the wind rotates from the initial northward direction to a direction 60° from north towards the east. It also appears that two lobes of the fallout pattern are formed due to variations in terrain elevation.

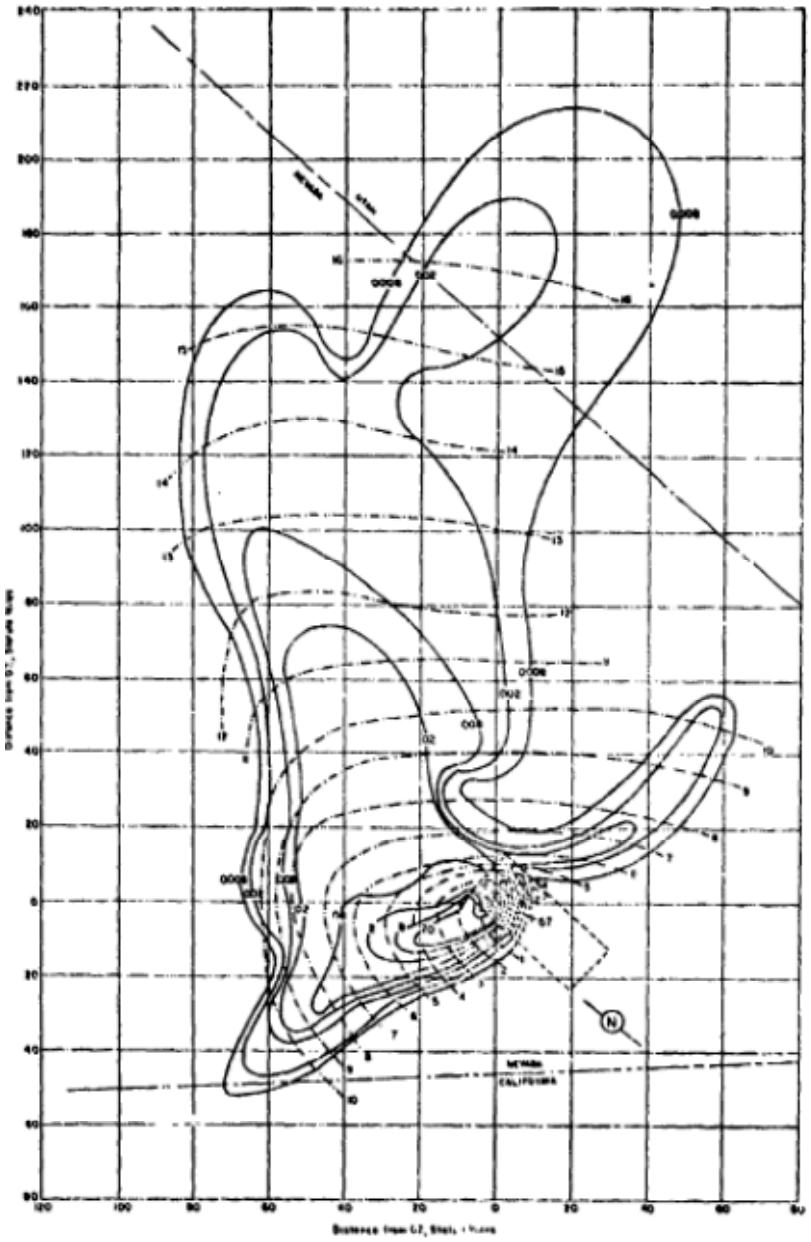

Figure 3-7. Ground-shine dose-rate contours for the NTS explosion Turk at H+1 hr in R/hr.

4.0 CONCLUSIONS AND RECOMMENDATIONS

The complexity of fallout footprints shown by our simulations using variations in meteorology suggest that accurate predictions of fallout will be difficult without well constrained estimates of the local meteorology. Uncertainty will be exacerbated by any lack of confidence in the environmental material (e.g., soil) properties and the detonation parameters such as yield and height of burst. These findings suggest that it would be very useful to better constrain the local meteorology as well as the near-source environmental material and detonation parameters. Once we have a better understanding of the range of probable model parameters we can focus on reducing uncertainties in those parameters that have the greatest impact on predicted fallout, and can also do a better job of estimating the range of possible fallout patterns.

The primary results from this study are as follows:

1. Fallout levels are non-linear functions of yield and height of burst with greater variation in levels for lower yields and smaller heights of burst.
2. Potential variations in fallout consistent with uncertainties in in-situ environmental material properties and the particle activity-size distribution model are potentially quite large. Our simulations with plausible but poorly constrained particle size distributions produced cases ranging from the majority of fallout being deposited near ground-zero, to being transported to relatively large distances downwind.
3. Better constraints on the in-situ particle size distribution model input parameters, particularly at low yields and heights of burs, are critical for producing reliable estimates of nuclear detonation fallout.
4. Uncertainties in meteorology are another potentially significant source of uncertainty in predicted fallout. For example, variation in wind direction as a function of height can lead to complicated multi-directional fallout footprints. Such fallout footprints are consistent with observations of fallout at NTS (Hawthorne, 1979).
5. Variations in wind speed as a function of height can have a significant effect on the relative amount of material that is deposited in the near-field and far-field downwind regions.
6. Precipitation scavenging can significantly increase ground deposition in areas of precipitation, and, then, reduce deposition downwind of the precipitation areas.
7. Topography can cause additional complexity in the fallout plumes, changing the direction of the plume, spatial distribution of the fallout, and the distances at which significant fallout occurs.
8. Sensitivity to topography depends on yield as well as local meteorology.

5.0 ACKNOWLEDGEMENT

The author would like to acknowledge John Nasstrom, Brenda Pobanz and Mike Kristo for their contributions to this project.

6.0 REFERENCES

Bridgman, C.J. and W.S. Bigelow, *A New Fallout Prediction Model, Health Physics*, **43**:205-218, August 1982.

DOE/NV-209, *United States nuclear tests, July 1945 through September 1992, Rev. 14*, U.S. Department of Energy, 1997

Freiling, E. C., *Radionuclide Fractionation in Bomb Debris*, *Science*, Vol 133, 1961

Goldstein, P., *Rapid Debris Analysis Project Task 3 Status Report – Sensitivity of Forensic Measurements to Source Parameters*, Lawrence Livermore National Laboratory, Livermore, CA, LLNL-TR-637992 May, 2013a.

Goldstein, P., *Rapid Debris Analysis Project Task 3 Status Report – Sensitivity of Fallout to Near-Detonation Environment Material Properties,* Lawrence Livermore National Laboratory, Livermore, CA, LLNL-TR-637992 May, 2013b.

Harvey, T., F. Serduke, L. Edwards, L. Peters, *KDFOC3: A Nuclear Fallout Assessment Capability*, Lawrence Livermore National Laboratory, UCRL-TM-222788, 1992.

Hawthorne, H.A. (editor), *Compilation of Local Fallout Data From Test Detonation 1945-1962 Extracted from DASA 1251 Volume I – Continental U.S. Tests,* (DNA 1351-1-EX), Defense Nuclear Agency, Washington DC, 619 pp., 1979.

Heft, R.E., *The Characterization of Radioactive Particles from Nuclear Weapons Tests*, Radionuclides in the Environment. Advances in Chemistry Series #93, American Chemical Society, Washington D.C., 1970.

Huebsch, I.O., *Turbulence, Toroidal Circulation and Dispersion of Fallout Particles from the Rising Nuclear Cloud*, USNRDL-TR-1054 (5 August 1966).

May, Michael M, Reza Abedin-Zadeh, Donald A. Barr, Albert Carnesale, Philip E. Coyle, Jay Davis, Bill Dorland, Bill Dunlop, Steve Fetter, Alexander Glaser, Ian D. Hutcheon, Francis Slakey, Benn Tannenbaum, *Nuclear Forensics: Role, State of the Art, Program Needs*, Joint working group American Physical Society and American Academy for the Advancement of Science, 2008.

Martin, C.R. *Fallout Fractionation in Silicate Soils,* Ph.D. Dissertation, AFIT/DS/PH/83-3, ADA159226. Air Force Institute of Technology (AU), Wright-Patterson AFB OH, December 1983.

McGahan, J.T., *Graybeard Fallout Report*, Science Applications International Corporation, McLean, VA, November 30, 2001

McGahan, J.T., E.J. Kownacki, *Sensitivity of Fallout Predictions to Initial Conditions and Model Assumptions*, DNA 3439F, December 1974, (AD/A-002464).

Morris, D.B.. *A predictive technique for forecasting the isotopic composition of radioactive fallout,* Ph.D. Dissertation, AFIT/DS/ENP/04-02, Air Force Institute of Technology (AU), Wright-Patterson AFB OH, December 2004.

Norment, H.G., *DELFIC: Department of Defense Fallout Prediction System. Volume I. Fundamentals,* Atmospheric Sciences Associates, Bedford, MA., December 31, 1979

Nasstrom, J. S., G. Sugiyama, R. L. Baskett, S. C. Larsen, M. M. Bradley, *The NARAC modeling and decision support system for radiological and nuclear emergency preparedness and response*, Int. J. Emergency Management, **4**, 524-550, 2007

Spriggs, G.D., K.B. Knight, R.C. Gostic, *Characterization of Activity-Size-Distribution of Nuclear Fallout*, Stockpile Stewardship Quarterly, V2, #1, May 2012.

Sugiyama, Gayle; Nasstrom, John; Pobanz, Brenda; Foster, Kevin; Simpson, Matthew; Vogt, Phil; Aluzzi, Fernando; Homann, Steve. *Atmospheric Dispersion Modeling: Challenges of the Fukushima Daiichi Response*, Health Physics: May 2012 - Volume 102 - Issue 5 - p 493–508

Tompkins, R.C., *Department of Defense Land Fallout Prediction System – Volume V: Particle Activity*, Defense Atomic Support Agency, U.S. Army Nuclear Defense Laboratory, Edgewood Arsenal, MD, NDL-TR-102, DASA 1800-V, AD832239, February 1968.

Tompkins, R.C., *Sensitivity Analysis of the Particle Activity Module,* BRL R 1523, AD 880 619, U.S. Army Ballistics Research Laboratory, Edgewood, MD, January 1971 (U).

THIS PAGE IS INTENTIONALLY LEFT BLANK.

APPENDIX A. ABBREVIATIONS AND ACRONYMS

Item	Description
LLNL	Lawrence Livermore National Laboratory
NARAC	National Atmospheric Release Advisory Center
NTS	Nevada Test Site
GRIDGEN	NARAC continuous terrain Grid Generator code
ADAPT	Atmospheric Data Assimilation and Parameterization Techniques code
LODI	Lagrangian Operational Dispersion Integrator code
KDFOC	K-Division Fallout Code

THIS PAGE IS INTENTIONALLY LEFT BLANK.